



A rational molecular design on choosing suitable spacer for better host materials in highly efficient blue and white phosphorescent organic light-emitting diodes

Lin-Song Cui, Yuan Liu, Qian Li, Zuo-Quan Jiang*, Liang-Sheng Liao*

Jiangsu Key Laboratory for Carbon-Based Functional Materials & Devices, Institute of Functional Nano & Soft Materials (FUNSOM), Collaborative Innovation Center of Suzhou Nano Science and Technology, Soochow University, Suzhou, Jiangsu 215123, China

ARTICLE INFO

Article history:

Received 25 January 2014

Received in revised form 26 February 2014

Accepted 18 March 2014

Available online 16 April 2014

Keywords:

Organic light-emitting diodes

White

Host materials

Carbazole

Spacer

ABSTRACT

A series of host materials, 3,3'-linked carbazole-based molecules have been designed with phenyl and biphenyl spacers. Their optical and electrical properties can be fine-tuning by the spacers. Their HOMO energy levels depend on HOMO distributions within the range of -5.64 to -5.96 eV. On the other hand, the three compounds have similar LUMO energy levels and triplet energies. Their thermal, photophysical, electrochemical and carrier mobilities properties were also systematically investigated. The relationship between the molecular structures and optoelectronic properties are discussed. A blue PHOLED device incorporating **PBCz** achieved a maximum external quantum efficiency, current efficiency, and power efficiency of 19.5%, 45.5 cd/A and 43.8 lm/W, respectively. Moreover a two-color, all-phosphor and single-emitting-layer WOLED hosted by **PBCz** was also achieved with a maximum external quantum efficiency, current efficiency and power efficiency of 24.6%, 76.3 cd/A and 69.4 lm/W respectively. Furthermore, we also utilized this versatile host for three-component RGB white PHOLEDs and show excellent performance. For example, combination of **PBCz** with Flrpic, Ir(ppy)₂(acac) and Ir(MDQ)₂(acac) in the active layer, the resulting WOLEDs showed three evenly separated peaks and gave a high efficiency of 49.2 cd/A. The efficient PHOLEDs demonstrated that the versatile host **PBCz** has great potential for applications in the solid-state lighting.

© 2014 Elsevier B.V. All rights reserved.

1. Introduction

With the emergence of organic semiconductor in the prosperous optoelectronic research, carbazole, a tricycle heteroaromatic compound, successfully catch the chemists' eyesight for its electron-active conjugated ring and the electron-donating property [1,2]. To date, considerable work has been studied on organic light-emitting diodes (OLEDs), organic photovoltaics (OPVs) or dye-sensitized

solar cells (DSCs) etc. by using carbazole derivatives [3–5]. One of the significant applications of carbazole is designing host materials in phosphorescent OLEDs, especially when the PHOLEDs are considered as the solution of low efficient fluorescent OLEDs, because it could achieve theoretical 100% internal quantum efficiency by utilizing both electrogenerated singlet and triplet excitons for emission [6–13].

The host materials, as the majority component, are doped with phosphor emitters (usually heavy-metal complexes, Ir, Pt or Os etc.) in the emitting layer of a prototypical PHOLED [14–16]. Moreover, the white PHOLEDs based on a versatile host doped with different color dopants have

* Corresponding authors. Tel.: +86 512 65880945; fax: +86 65882846.
E-mail addresses: zqjiang@suda.edu.cn (Z.-Q. Jiang), lslliao@suda.edu.cn (L.-S. Liao).

attracted great attention because of its relatively simple and more cost effective fabrication processes [17–24]. On the other hand, the host–guest system is indispensable to avoid triplet polaron quenching (TPQ) and triplet–triplet annihilation (TTA) and realize the improvement of light-emitting quantum yields via efficient energy-transfer [25–29]. In this research field, carbazole-based materials can easily fulfill the basic requirements of suitable hosts, such as: (1) higher triplet energy (E_T), (2) matched HOMO/LUMO levels, (3) good thermal stability, and (4) good carrier mobility [30–37].

For the green or red phosphorescence, many carbazole-based hosts can qualify for good performance [38,39]. But for blue phosphorescence, the selection for good hosts becomes much more limited, and need more rational molecular design on how to find the balance between the high triplet energy (above 2.70 eV) and other requirements. Nevertheless, the combination of functional groups often leads to π -conjugation enlargement of host materials, which would accordingly reduce their triplet energies [40]. Hence, to obtain high triplet energies for host materials, the π -conjugation in the host molecules must be minimized. The design strategies such as using *meta* or *ortho*-linkage ways, non-conjugation building blocks or steric groups to limit the π -conjugation are usually employed [41–47]. As to the factually basic building block of *N*-phenyl-9H-carbazole (**PCz**), there are several linking ways to expand the molecular system to be an appropriate host material. Recently, we have done a series of systematic work to disclose the relationship between the molecular topology and physical properties of the host material to develop better high triplet host materials for blue and white PHOLEDs. The three simple isomers (**CTP-1**, **CTP-2** and **CTP-3**) by using one biphenyl group to separate two **PCz** groups with different linkage ways [48]. Our method is based on the fact that appending one more phenyl ring from the 3-position of the carbazole will not significantly reduce its triplet energy, and furthermore, it may bring better hole-mobility because of the longer HOMO distribution. Though, the **CTP-1** is a good host material as compared to its isomers and other traditional carbazole-based hosts. We believe that it can be further improved by carefully modifying the structure by continuing our design rule.

In this paper, we would like to develop better host material by reinvestigating the HOMO and LUMO distribution of **CTP-1**, and on this basis, we proposed that using one phenyl ring to replace biphenyl ring may be a better choice because of more suitable HOMO/LUMO level and higher carrier mobility. The resulted new material 1,3-bis(9-phenyl-9H-carbazol-3-yl) benzene (**PBCz**), was synthesized by one-step reaction and used in PHOLEDs as host for blue and white emission. When using **PBCz** as host and Irpic and PO-01 as dopants, the maximum power efficiencies can reach 43.8 and 69.4 lm/W in the blue and warm white PHOLEDs, which are higher than those in the corresponding **BCzPh** and **CTP-1**-based devices. Although high in efficiency, these devices show low color rendering index and poor coordinates, which is insufficient for illumination sources. To solve this problem, we also utilized this versatile host for three-component RGB white

PHOLEDs and show excellent performance. Upon combination of **PBCz** with Irpic, Ir(ppy)₂(acac) and Ir(MDQ)₂(acac) in the active layer, the resulting WOLEDs showed three evenly separated peaks and gave a high efficiency of 49.2 cd/A (46.5 lm/W, 19.1%). The RGB WOLEDs demonstrated high efficiency and proper CIE coordinates for solid-state lighting.

2. Results and discussions

2.1. Synthesis and characterization

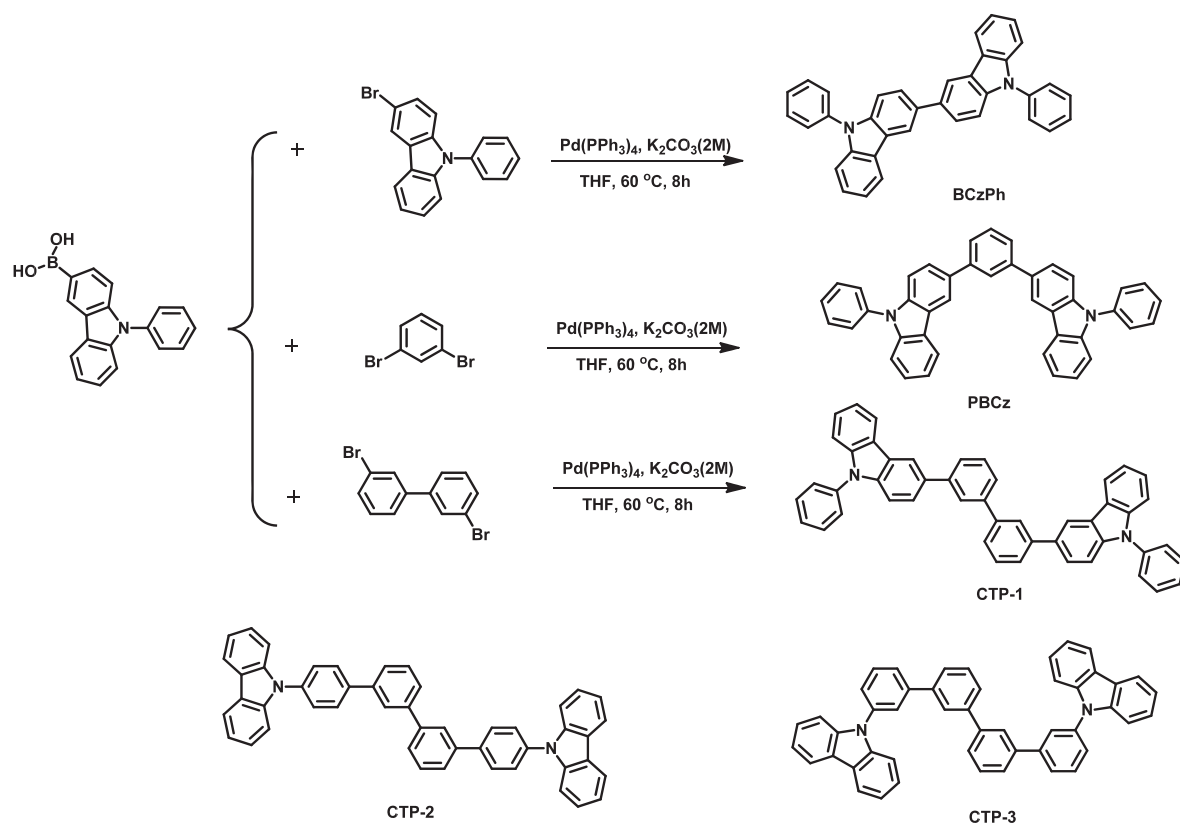
The synthetic routes and chemical structures of the three hosts are shown in Scheme 1. The new host **PBCz** was facilely prepared through classic Suzuki–Miyaura cross coupling reaction from *N*-phenylcarbazole-3-boronic acid with 1,3-dibromobenzene in high yields. The start material 1,3-dibromobenzene is easier to attainable and could reduce the process time and cost of **PBCz**. Afterwards, **PBCz** was further purified by repeated temperature gradient vacuum sublimation. Its chemical structure was fully characterized by ¹H NMR and ¹³C NMR spectroscopies, mass spectrometry and elemental analysis. The detailed synthetic methods and analysis are described in the Experiment Section.

2.2. Thermal properties

The thermal property of **PBCz** was investigated through thermogravimetric analysis (TGA) and differential scanning calorimetry (DSC) and the data of **BCzPh** and **CTP-1** are also presented for comparison, which are summarized in Table 1. As shown in Fig. 1, the **PBCz** exhibited clear glass transition under heating at 115 °C, which is 13 °C higher than that of **BCzPh** and 8 °C lower than that of **CTP-1**. The decomposition temperature (T_d) with 5% loss is estimated to be 409 °C (Fig. S1). This suggests that **PBCz** could form morphologically stable and uniform amorphous films by vacuum deposition for OLED fabrication.

2.3. Photophysical properties

Fig. 2 show the UV–Vis absorption and fluorescence (PL) spectra of **BCzPh**, **PBCz** and **CTP-1** in dilute CH₂Cl₂ solution, as well as the phosphorescence (Phos) spectra measured in a frozen 2-methyltetrahydrofuran matrix at 77 K. The absorption around the 270–300 nm of the three materials are associated with the π – π^* transitions of the carbazole units and the absorption in the range of 325–355 nm can be assigned to the n – π^* electron transition of the entire conjugated backbone. Upon photoexcitation at the absorption maximums at room temperature, the fluorescent spectra of **PBCz** and **CTP-1** are nearly identical to each other, but different from the spectrum of **BCzPh**. The emission peaks of **PBCz** and **CTP-1** exhibit ~30 nm hypochromatic shift as compared to that of **BCzPh**. This assignment implied that inserting one phenyl or biphenyl can trail off the interaction between the two **PCz** units. The E_T of **BCzPh** and **CTP-1** were determined by the highest energy vibronic band of the



Scheme 1. Molecular structures and synthesis of BCzPh, PBCz and CTP-1~3.

Table 1

Physical Properties of BCzPh, PBCz and CTP-1.

Compound	T_g^a (°C)	T_d^a (°C)	λ_{abs}^b (nm)	λ_{em}^b (nm)	λ_{ph}^c (nm)	E_g^d (eV)	E_T^e (eV)	HOMO/LUMO ^f (eV)	Hole mobility ^g (cm ² V ⁻¹ S ⁻¹)
BCzPh	100	340	303	393, 408	452	3.37	2.74	5.64/2.36	2.93×10^{-5}
PBCz	115	409	289	362, 381	450	3.41	2.76	5.86/2.40	3.62×10^{-5}
CTP-1	123	448	289	365, 380	448	3.49	2.77	5.96/2.43	1.18×10^{-5}

^a T_g : glass transition temperatures.

^b Measured in dichloromethane solution at room temperature.

^c Measured in 2-MeTHF glass matrix at 77 K.

^d E_g : The band gap energies were estimated from the optical absorption edges of UV–Vis absorption spectra.

^e E_T : The triplet energy were estimated from the onset peak of the phosphorescence spectra.

^f HOMO levels were estimated from cyclic voltammetry, LUMO levels were calculated from HOMO and E_g .

^g Mobility was calculated from space charge limited current.

phosphorescence spectra as *ca.* 2.75 eV and 2.76 eV, respectively, which is almost identical to that of **BCzPh** (2.75 eV), implying that the introduction of a phenyl or biphenyl between two **PCz** does not alter the triplet energy. This may due to the *meta–meta* configuration of the entire molecules. That also means it is feasible to fix T_1 and simultaneously tune S_1 in such simple ways. The triplet energies of **PBCz** and **CTP-1** are sufficiently high to serve as host materials for blue and white PHOLEDs.

The absorption spectrum of the phosphorescent dopant is compared in Fig. S2 with the solid emission spectra (PL) of the three hosts. Iridium(III) bis[(4,6-difluorophenyl)pyridinato-N, C^{2'}] picolinate (Flrpic, $E_T = 2.65$ eV) serves as the emitter, with a lower T_1 level than that of

the three hosts. However, The overlap between the PL spectrum of the **PBCz** and **CTP-1** and the absorption of the Flrpic are larger than that of **BCzPh**. Hence, the energy transfer from the **PBCz** and **CTP-1** to the Flrpic should be more efficient in the host–guest system. This indicates that the hosts **PBCz** and **CTP-1** maybe show better performance than that of **BCzPh** in host–guest system PHOLEDs.

2.4. Energy levels and molecular design

The electrochemical behaviors of **BCzPh**, **PBCz** and **CTP-1** were probed by cyclic voltammetry in deoxygenated CH₂Cl₂ with ferrocene as the internal reference (see Fig. 3), and they all displayed irreversible oxidation process. The

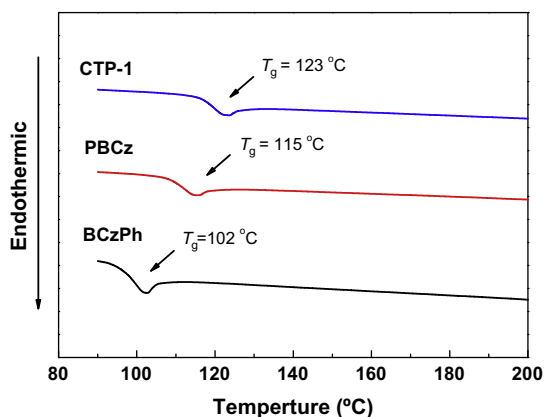


Fig. 1. TGA curves of BCzPh, PBCz and CTP-1.

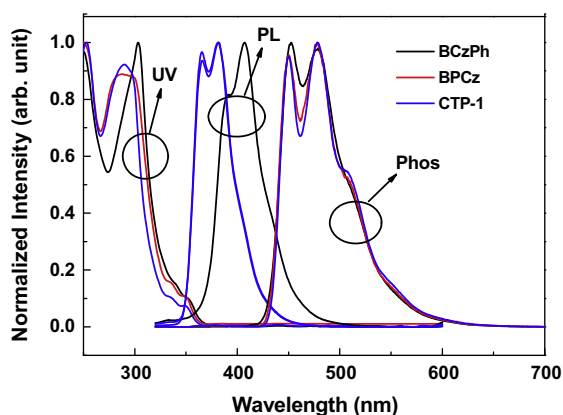


Fig. 2. Room-temperature UV-Vis absorption and fluorescence (PL) spectra of BCzPh, PBCz and CTP-1 in CH_2Cl_2 solution and phosphorescence (Phos) spectra measured in a frozen 2-methyltetrahydrofuran matrix at 77 K.

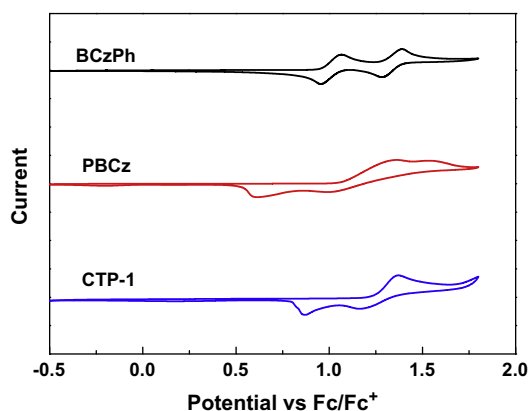


Fig. 3. Cyclic voltammograms of BCzPh, PBCz and CTP-1 in dichloromethane solution for oxidation.

HOMO energy levels were estimated from the onset of oxidation potentials relative to the vacuum level. The HOMO

level of **BPCz** and **CTP-1** were -5.86 eV and 5.96 eV, respectively, which were $0.22/0.26$ eV and $0.32/0.36$ eV lower than **BCzPh** (-5.64 eV)/Flrpic (-5.60 eV). These values indicate that the **BPCz** and **CTP-1** hosts can probably enhance hole-trapping on the guest Flrpic and thus improve the device performance [49]. The optical band gap (E_g) of **BCzPh** and **CTP-1** are 3.45 eV and 3.47 eV, which are calculated from the threshold of the absorption spectra in CH_2Cl_2 solution. The LUMO levels of **PBCz** and **CTP-1** are determined as -2.40 eV and -2.43 eV, respectively, according to the equation $E_{\text{LUMO}} = E_{\text{HOMO}} + E_g$. In comparison with **BCzPh** (LUMO = -2.36 eV), the LUMO energy levels of three compounds are nearly the same. These will be detail discussed in the following section.

In order to better understand the effects of phenyl and biphenyl spacer on the spatial distribution of their HOMO and LUMO, density functional theory (DFT) calculations were performed for **PBCz** and **CTP-1** using B3LYP hybrid functional theory with Gaussian 09. The structure of **BCzPh** was also calculated for comparison under identical conditions. Fig. 4 illustrates the HOMO and LUMO distributions for **BCzPh**, **PBCz** and **CTP-1**. For **BCzPh**, both HOMO and LUMO are mostly localized at the dicarbazole backbone with little contribution from the peripheral phenyl moiety. However, with insertion of an additional phenyl (**PBCz**) or biphenyl group (**CTP-1**) in the **BCzPh** conjugated backbone, the HOMOs are not only localized at the two **PCz** units but also spread over the phenyl or biphenyl spacer. But the LUMOs still concentrated in the carbazole ring. The obvious separation between HOMOs and LUMOs in **PBCz** and **CTP-1** indicate that the one-electron HOMO–LUMO transition would become a typical charge-transfer (CT) transition, which is preferable for efficient hole- and electron-transporting properties and the prevention of reverse energy transfer. Interestingly, the fact that the HOMOs of **BCzPh**, **PBCz** and **CTP-1** molecules are localized on different subunits and can present higher and lower HOMO energy levels. On the one hand, as the HOMO of the **BCzPh** consists primarily of the π orbital of the dicarbazole unit. In order to obtain more information about the HOMOs for **BCzPh**, **PBCz** and **CTP-1**, the molecular orbital compositions of these molecules were calculated [50,51]. The electron density of the HOMO is mainly localized on the carbazoles with dominating contributions (72.75–91.06%), suggesting that the HOMOs of the three molecules are determined mostly by the carbazole unit. In other words, the additional phenyl/ biphenyl unit of **PBCz/CTP-1** also have some contributions in **PBCz** and **CTP-1** molecules. For the two molecules, the contributions of the carbazole groups to the HOMO are smaller than that in corresponding **BCzPh**, with a decrease about 18%, leading to higher HOMOs for the **BCzPh** than that for the **PBCz** and **CTP-1**. Hence, the HOMO energy levels increase in the order: **CTP-1** (-5.21 eV) < **PBCz** (-5.17 eV) < **BCzPh** (-4.96 eV). The result is predicted to lower the HOMO levels, which was consistent with the cyclic voltammetry measurements and UPS data (see the Supporting Information). Furthermore, the LUMO energies of the three molecules are close because the LUMO shows similar distributions. The electron density in the LUMOs of **BCzPh**, **PBCz** and **CTP-1** is primarily located on the biphenyl of two

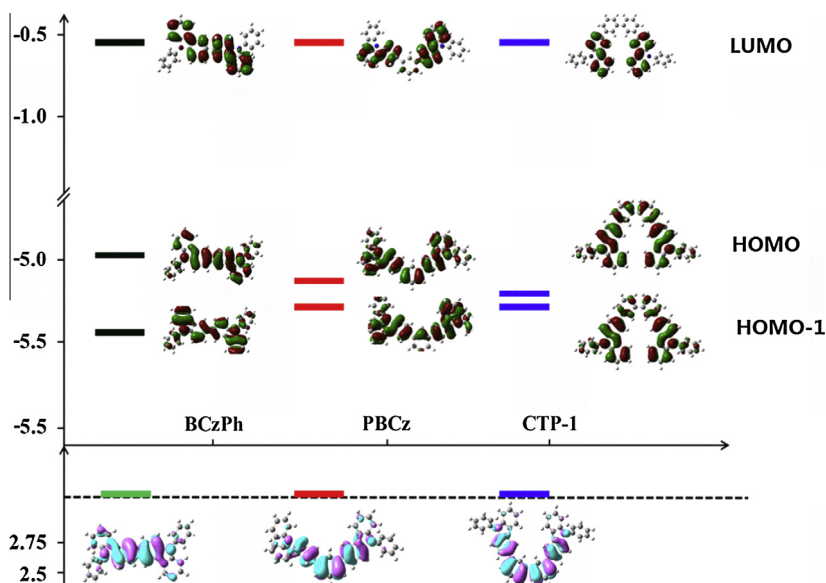


Fig. 4. Frontier molecular orbitals (FMOs) distribution (above) and spin density distributions of the T_1 values (below) for BCzPh, PBCz and CTP-1 calculated with DFT at the B3LYP/6-31G(d) level.

carbazole function groups. Therefore, there is little change in the LUMO levels upon by inserting a phenyl or biphenyl between two PCz units of the BCzPh molecule. From the calculated and experiment results, the point to emphasize is that the HOMOs of the PBCz and CTP-1, are lower than that of BCzPh, which would make efficient hole trap when used as host materials. The HOMOs of PBCz and CTP-1 can be independently turned by chemical modification of phenyl/biphenyl spacer with little effect LUMO energy levels, and this will greatly facilitate the molecular design and property control of these materials.

As mentioned in introduction, efficient PHOLEDs need to suppress the back energy transfer from guest to host so that the triplet energy of the host must be higher than that of the guest. The calculated triplet energies of the three hosts are collected in Table S1. The theoretical results are in good agreement with experiment and confirm that the phenyl and biphenyl spacer do not alter the triplet energy of BCzPh molecule. This may be due to the π -conjugation are not extended because of the *meta*-configuration and the *meta*-substitution. A further confirmation comes from the NTO (natural transition orbital) analyses, carried out on the basis of the optimized T_1 -state geometries of the three hosts and illustrated in Fig. 6 below. The hole-particle NTOs for PBCz and CTP-1 were interrupted by phenyl and biphenyl spacer. For PBCz it is divided into two parts: biphenyl and phenyl segment. For CTP-1 it is comprised of two biphenyl segments. Obviously, the hole-particle NTOs for BCzPh are localized on a biphenyl segment. Resultantly, the three hosts are found to have similar triplet energy. However, phenyl and biphenyl spacer hardly affected the triplet energy due to the similar nature of the triplet state. On the other hand, in the cases of PBCz and CTP-1, a phenyl or biphenyl group is inserted between the two PCz groups and actually serves as a buffer to keep the high triplet energy.

2.5. Hole transport properties

We also studied the carrier-transport properties of the three materials using hole-only device with the structure of ITO/MoO₃ (20 nm)/host (100 nm)/MoO₃ (20 nm)/Al (100 nm). It can be assumed that only holes are injected and transported in the devices because the work function of MoO₃ is high enough to block electron injection. Fig. 5 shows the current density versus voltage characteristics of the hole-only devices. Here, the BCzPh-based and PBCz-based hole-only device shows the more efficient hole injection and transport than BCzPh-based device. The slopes, referring to the trap-free space-charge-limited-current region [52], are about 2.2 for the three hole-only devices. According to the Mott–Gurney law $J_{SCLC} = \frac{9}{8} \epsilon_0 \epsilon_r \mu \frac{V^2}{d^3}$, the mobilities of the three hosts are estimated and summarized in Table 1.

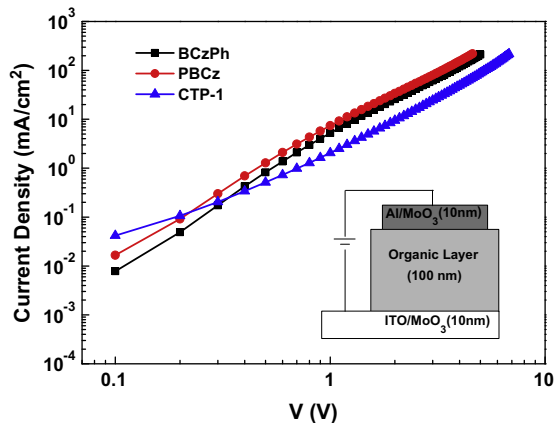


Fig. 5. Current density versus voltage characteristics of the hole-only devices consisting of BCzPh, PBCz and CTP-1 layers.

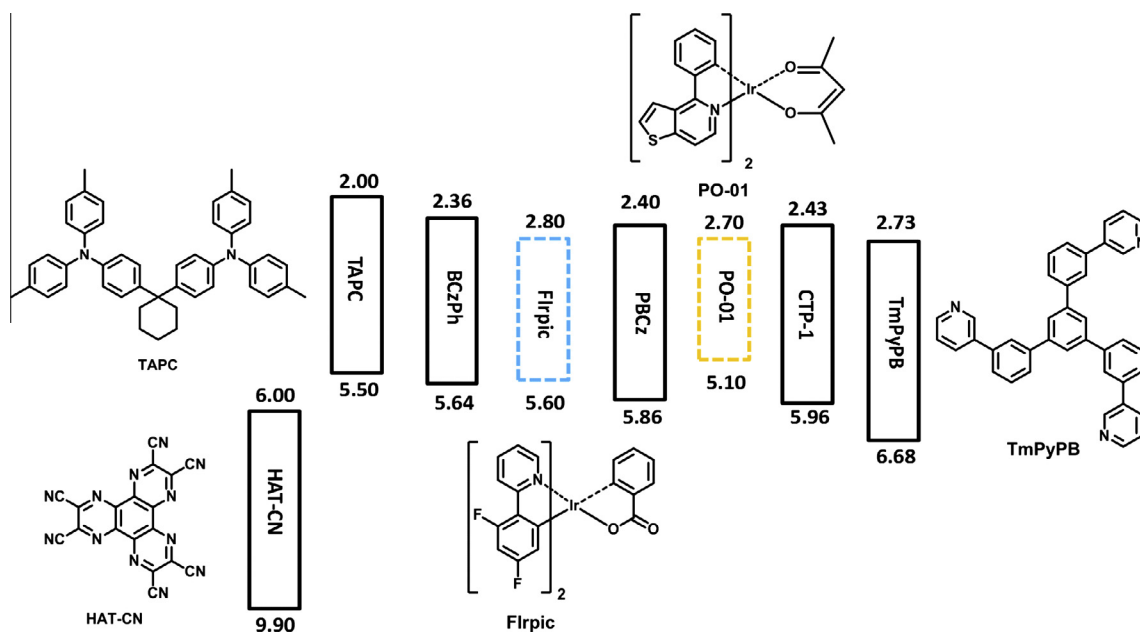


Fig. 6. Energy levels of the materials employed in the devices.

2.6. Electroluminescence of OLEDs

In order to evaluate the potentials of **PBCz** and **CTP-1** as host materials for the sky blue phosphor **Flrpic**, the devices were fabricated with typical sandwiched structures by sequential vapor deposition of the materials onto a glass substrate coated with ITO. We utilized strongly electron-deficient 1,4,5,8,9,11-hexaazatriphenylene-hexacarbonitrile (**HAT-CN**) as hole-injection layer (HIL), 1,1-bis[4-[N,N-di(p-tolyl)amino]phenyl]cyclohexane (**TAPC**) as hole-transporting layer (HTL) and electron-blocking layer. 1,3,5-tri[(3-pyridyl)-phen-3-yl]benzene (**TmPyPB**) was used as electron-transporting as well as hole-blocking layer. 8-Hydroxyquinolinolato-lithium (**Liq**) served as electron-injecting layer and Al acted as cathode. The **Flrpic**-doped devices were fabricated with a simple configuration of ITO/**HAT-CN** (10 nm)/**TAPC** (45 nm)/Host: **Flrpic** (5 wt%, 20 nm)/**TmPyPB** (50 nm)/**Liq** (2 nm)/Al (120 nm) (Host = **BCzPh**: device BA; Host = **PBCz**: device BB; Host = **CTP-1**: device BC). The emitting material layers are the newly prepared **Flrpic**-doped **PBCz** or **CTP-1**. Meanwhile, the control devices using **BCzPh** (device BA) as hosts

were also fabricated. The best electroluminescence (EL) performance was achieved with 5 wt.% **Flrpic** for the hosts. Fig. 6 depicts the relative energy levels of the materials employed in the devices. All the devices performance is summarized in Table 2.

The current density–voltage–brightness (*J–V–L*) characteristics and current efficiency, power efficiency and external quantum efficiency versus current density characteristics of the devices are shown in Fig. 7. All the devices show similar EL spectra. The EL spectra of the **BCzPh**, **PBCz** or **CTP-1**-based devices show identical patterns to **Flrpic** emission without any emission from the host and/or adjacent layer. The EL results indicate that the perfect energy transfer from host to **Flrpic** generate upon electrical excitation, and charge carriers and excitons are completely confined in the emitting layer. Generally, **Flrpic** is a sky-blue emitter with a typical maximum emission peak around 472 nm and a shoulder peak at 500 nm, with a CIE (*x, y*) around (0.15, 0.37).

As illustrated in Fig. 7, device BC hosted by **CTP-1** exhibited a maximum current efficiency ($\eta_{c, \max}$) of 40.5 cd/A, a maximum power efficiency ($\eta_{p, \max}$) of 33.9 lm/W and a

Table 2
Electroluminescence characteristics of the devices.

Device	Host/guest	V^a (V)	η_c^b (cd/A)	η_p^b (lm/W)	η_{ext}^b (%)
BA	BCzPh/Flrpic	3.2	36.5, 35.7, 24.2	35.5, 6.5, 3.3	15.6, 15.3, 10.3
BB	PBCz/Flrpic	3.4	45.5, 45.4, 43.7	43.8, 43.7, 33.6	19.5, 19.4, 18.7
BC	CTP-1/Flrpic	4.7	40.5, 40.4, 38.2	33.9, 17.2, 10.0	17.3, 17.3, 16.3
WA	BCzPh/Flrpic + PO-01	3.5	55.8, 55.8, 53.6	49.0, 49.0, 38.0	17.8, 17.8, 17.2
WB	PBCz/Flrpic + PO-01	3.4	76.2, 76.2, 73.6	69.4, 69.4, 55.0	24.6, 24.6, 23.6
WC	CTP-1/Flrpic + PO-01	3.5	67.4, 67.4, 64.6	60.2, 60.2, 45.9	21.5, 21.5, 20.7
WD	PBCz/B + G + R	3.2	49.0, 48.5, 48.6	46.3, 46.3, 36.8	19.1, 18.9, 19.0

^a Voltage (V) at 100 cd/m².

^b Current efficiency (η_c), power efficiency (η_p) or external quantum efficiency (η_{ext}) in the order of maximum, at 100 cd/m² and at 1000 cd/m².

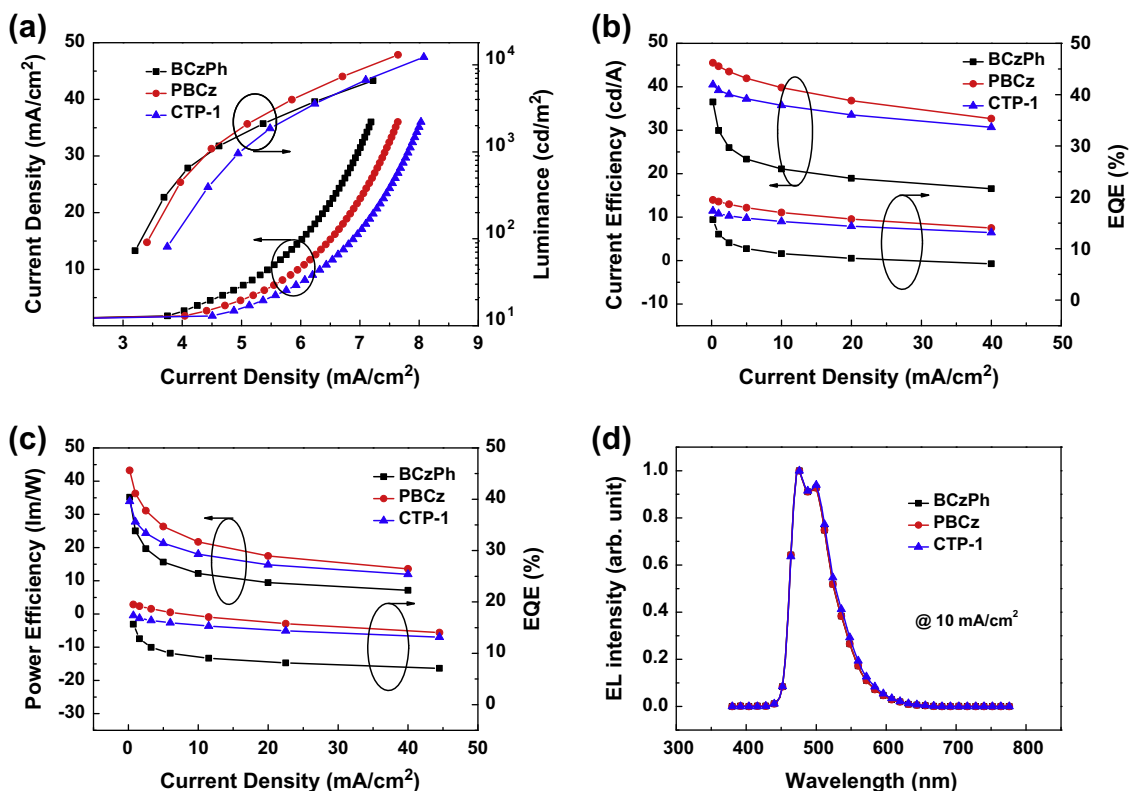


Fig. 7. (a) Current density–voltage–luminance characteristics, (b) current efficiency and external quantum efficiency versus current density curves, (c) power efficiency and external quantum efficiency versus current density curves and (d) the EL spectrum of devices BA–BC at 10 mA/cm².

maximum external quantum efficiency ($\eta_{\text{ext, max}}$) of 17.3%. The same trend can be observed for devices B. Device BB hosted by **PBCz** displays substantially higher efficiencies with $\eta_{\text{c, max}}$ of 45.5 cd/A, $\eta_{\text{p, max}}$ of 43.8 lm/W and $\eta_{\text{ext, max}}$ of 19.5%. In comparison, the control device BA using **BCzPh** as the host exhibits lower efficiencies ($\eta_{\text{c, max}}$ of 36.5 cd/A, $\eta_{\text{p, max}}$ of 35.1 lm/W and $\eta_{\text{ext, max}}$ of 15.6%). These values are higher than that of the comparable blue device using conventional host *mCP*, which achieves $\eta_{\text{c, max}}$ of 34.5 cd/A, $\eta_{\text{p, max}}$ of 23.1 lm/W and $\eta_{\text{ext, max}}$ of 13.7% (Fig. S6). On the other hand, the drive voltage (at the luminance of 100 cd/m²) of the device BA hosted by **BCzPh** was 3.3 V, which is lower than that of device BB by 0.2 V. The current density of device BA is also higher than that of device BB at the same voltage. Interestingly, it is worth noting that the devices BB and BC show low EQE roll-offs. Remarkably, when the brightness reached 1000 cd/m², the EQEs still remained as high as 18.7% and 16.4% for devices BB and BC, respectively, while the EQE of device BA dropped to 10.3%. It could be attributed to the different HOMO energy levels of the host materials. As depicted in Fig. 6, **BCzPh** (−5.64 eV) has similar HOMO level with Flrpic (−5.60 eV). In contrast, **PBCz** (−5.86 eV) is 0.25 eV lower than Flrpic, which may be inclined to format dopant trapping effect. For **BCzPh**-based device, holes are directly transported on the host while for **PBCz**-based device, parts of the holes are trapped on the dopant. Considering the excellent electron transport property of Flrpic, this will

lead to a broader recombination zone in **PBCz**-based device compared to **BCzPh**-based device.

In addition, to further evaluate their suitability for white PHOLEDs, the all phosphor two-color white OLEDs have been fabricated with the configuration of ITO/HAT-CN (10 nm)/TAPC (45 nm)/Host: Flrpic: PO-01 (5%, 0.5%, 20 nm)/TmPyPB (40 nm)/Liq (2 nm)/Al (120 nm) (Host = **BCzPh**: device WA; Host = **PBCz**: device WB; Host = **CTP-1**: device WC). Flrpic and PO-01 were co-doped into the three hosts as emitting material layer. Fig. 8 shows the curves of external quantum efficiency, power efficiency and external quantum efficiency versus current density. The devices WA–WC obtained the $\eta_{\text{c, max}}$ of 55.8, 76.2, 67.4 cd/A, $\eta_{\text{p, max}}$ of 49.0, 69.4, 60.2 lm/W and $\eta_{\text{ext, max}}$ of 17.8, 24.6, 21.5% respectively. Moreover, the emission color of these devices exhibited stability and varied slightly from (0.36, 0.48) at 4 V to (0.34, 0.47) at 8 V. Similar to the blue PHOLEDs, the current/power efficiencies of the devices hosted by these materials are in the order device WB > device WC > device WA, which also demonstrates the superiority of **PBCz**. But, the lack of red peaks in the spectrum leads to a poor CIE coordinates.

In this regards, we then studied the incorporation of RGB three-color emitters in the white devices. The device structure was ITO/HAT-CN (10 nm)/TAPC (45 nm)/**PBCz**: Flrpic (5%, 19 nm)/**PBCz**: Ir(ppy)₂(acac): Ir(MDQ)₂(acac) (3%, 1%, 1.5 nm)/ TmPyPB (40 nm)/Liq (2 nm)/Al (120 nm), where 19 nm-thick **PBCz** doped with 5 wt.%

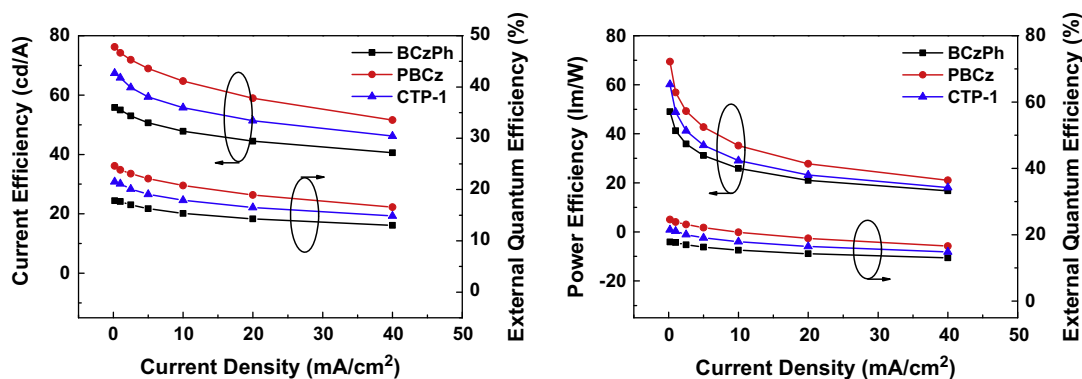


Fig. 8. (a) current efficiency and external quantum efficiency versus current density curves, (b) power efficiency and external quantum efficiency versus current density curves.

Flrpic served as the blue-emitting layer and 1.5 nm 3 wt.% Ir(ppy)₂(acac) and 1% Ir(MDQ)₂(acac) were co-doped into PBCz worked as the green–red-emitting layer. The EL characteristics of device WD are shown in Fig. 9 and the respective data are summarized in Table 2. The resulting white spectra exhibited three main peaks centered at 475 nm, 516 nm and 596 nm, which arose from the emission of the Flrpic, Ir(ppy)₂(acac) and Ir(MDQ)₂(acac), respectively. The spectra also demonstrated moderate color stability. With the increase of driving voltage, the intensity of blue and red peaks decreased slightly with the CIE coordinates changing from (0.45, 0.42) at 3.0 V to (0.44, 0.43). The device performances were achieved to be $\eta_{c, \max}$ of 49.2 cd/A, $\eta_{p, \max}$ of 46.5 lm/W and $\eta_{\text{ext}, \max}$ of 19.1%, respectively. When these WOLEDs are applied to solid-state lighting, all of the photons should be taken into account for illumination because the originally trapped photons can be redirected to the forward-viewing direction by applying light out-coupling techniques such as by roughing the substrate, patterning a micro-lens array or engineering the lighting fixtures [53]. It has been experimentally demonstrate that the efficiency can be improved by a factor of 1.2–2.3 if certain light out-coupling techniques are used. In this regards, a maximal total current efficiency of ≈ 88.6 cd/A can be obtained if a factor of 1.8 is adopted. The results indicated that PBCz can be used as host material for white PHOLEDs

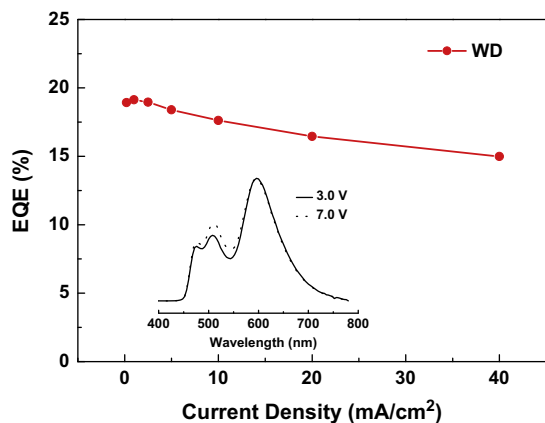


Fig. 9. Current efficiency and external quantum efficiency versus current density curves, The inset is the EL spectra of device WD at 3 V and 7 V.

with high efficiency and proper CIE coordinates for solid-state lighting. On the other hand, the color rendering index (CRI) of three-color white PHOLEDs (CRI = 76) are better than that of two-color white PHOLEDs (CRI = 47).

3. Conclusion

In summary, an evolution of carbazole-based host materials is presented in this paper. After constructing a series of carbazole-based compounds previously to reveal the optimized linking position to modify required properties for blue host materials, we reach the concept of how to control the T_1 distribution to get sufficient triplet energy. A simple carbazole-based host material, namely PBCz, for PHOLEDs has been designed and synthesized by inserting one phenyl ring between the two PCz units. This structure can endow it with sufficiently high thermal/morphological stabilities though the corresponding T_d/T_g is slightly lower than that of CTP-1. Compared to CTP-1, the subtraction from biphenyl group to one phenyl group could effectively tune the HOMO energy level and improve hole-mobility, while maintaining high triplet energy. Blue and warm-white PHOLEDs were fabricated using PBCz as hosts and Flrpic/PO-01 as dopants, which exhibited enhanced efficiencies with low roll-off. Specifically, the current efficiencies of PBCz-based devices can reach 45.5 cd/A and 76.2 cd/A at 100 cd/m² in blue and white PHOLEDs, which were superior to those of CTP-1-based devices. Moreover, upon combination of PBCz with Flrpic, Ir(ppy)₂(acac) and Ir(MDQ)₂(acac) in the active layer, the three colors WOLEDs demonstrated a high EQE of 19.1% and a proper CIE coordinates of (0.45, 0.42). This is a rational molecular design on how to investigate the more suitable materials by considering position and spacer effects to tune the key factors for final device performances.

4. Experimental section

4.1. Materials and methods

All chemicals i.e., (9-phenyl-9H-carbazol-3-yl) boronic acid, [4-(9H-carbazol-9-yl) phenyl] boronic acid, [3-(9H-carbazol-9-yl)phenyl] boronic acid, 1-bromo-3-iodobenzene, 3-Bromobenzeneboronic acid were purchased from

Bepharmlimited and Alfa Aesar. And all of materials used without further purification. The important intermediates 3,3'-dibromodiphenyl was prepared according to the literature methods [31]. THF was purified by PURE SOLV (Innovative Technology) purification system. Chromatographic separations were carried out by using silica gel (200–300 nm). All other reagents were used as received from commercial sources unless otherwise stated. ^1H NMR and ^{13}C NMR spectra were recorded on a Varian Unity Inova 400 spectrometer at room temperature. Mass spectra were recorded on a Thermo ISQ mass spectrometer using a direct exposure probe. UV–Vis absorption spectra were recorded on a Perkin Elmer Lambda 750 spectrophotometer. PL spectra and phosphorescent spectra were recorded on a Hitachi F-4600 fluorescence spectrophotometer. Transient PL decays were measured by a single photon counting spectrometer from HORIBA JOBIN YVON with a Nano LED pulse lamp as the excitation source. Differential scanning calorimetry (DSC) was performed on a TA DSC 2010 unit at a heating rate of $10\text{ }^\circ\text{C}/\text{min}$ under nitrogen. The glass transition temperatures (T_g) were determined from the second heating scan. Thermo gravimetric analysis (TGA) was performed on a TA SDT 2960 instrument at a heating rate of $10\text{ }^\circ\text{C}/\text{min}$ under nitrogen. Temperature at 5% weight loss was used as the decomposition temperature (T_d). Cyclic voltammetry (CV) was carried out on a CHI600 voltammetric analyzer at room temperature with a conventional three-electrode configuration consisting of a platinum disk working electrode, a platinum wire auxiliary electrode, and an Ag wire pseudo-reference electrode with ferrocenium–ferrocene (Fc⁺/Fc) as the internal standard. Nitrogen-purged dichloromethane was used as solvent for the oxidation scan and DMF for the reduction scan with tetrabutylammonium hexafluorophosphate (TBAPF6) (0.1 M) as the supporting electrolyte. The cyclic voltammograms were obtained at a scan rate of $100\text{ mV}/\text{s}$.

4.2. Computational methodology

The geometrical and electronic properties of **BCzPh**, **PBCz** and **CTP-1** were performed with the Gaussian 09 program package. The calculation was optimized by means of the wb97xd (Becke three parameters hybrid functional with Lee–Yang–Perdew correlation functionals) with the 6-311G(d) atomic basis set. Molecular orbitals were visualized using Gaussview.

4.3. Fabrication of OLEDs

The OLEDs were fabricated through vacuum deposition of the materials at $ca. 2 \times 10^{-6}$ Torr onto ITO-coated glass substrates having a sheet resistance of $ca. 30\ \Omega$ per square. The ITO surface was cleaned ultrasonically – sequentially with acetone, ethanol, and deionized water, then dried in an oven, and finally exposed to UV-ozone for about 30 min. Organic layers were deposited at a rate of 2–3 Å/s, subsequently, Liq was deposited at 0.2 Å/s and then capped with Al ($ca. 4\ \text{Å}/\text{s}$) through a shadow mask without breaking the vacuum. For all the OLEDs, the emitting areas were determined by the overlap of two electrodes as 0.09 cm^2 . The EL spectra, CIE coordinates and J – V – L curves

of the devices were measured with a PHOTO RESEARCH SpectraScan PR 655 photometer and a KEITHLEY 2400 SourceMeter constant current source at room temperature. The EQE values were calculated according to the previously reported methods [54].

9,9'-diphenyl-9H,9'H-3,3'-bicarbazole (BCzPh): 3-bromo-9-phenyl-9H-carbazole (1.50 g, 4.66 mmol), 9-phenyl-9H-carbazol-3-ylboronic acid (1.47 g, 5.13 mmol) and tetrakis(triphenylphosphine)palladium(0) (0.26 g, 0.23 mmol) were dissolved in THF/2 M K_2CO_3 (3/1, v/v). The reaction mixture was heated to $60\text{ }^\circ\text{C}$ for 8 h under an argon atmosphere. After cooling to room temperature, the organic layer was separated and evaporated to remove solvent. The residue was purified by column chromatography with 1:3 (v/v) dichloromethane/petroleum ether as the eluent and recrystallized from dichloromethane/petroleum to give a white crystalline powder (1.92 g, 85%). ^1H NMR (400 MHz, CDCl_3) δ (ppm): 8.46 (s, 2H) 8.25 (d, $J = 8.0\text{ Hz}$, 2H) 7.79 (d, $J = 8.0\text{ Hz}$, 2H) 7.67–7.59 (m, 8H) 7.54–7.44 (m, 8H) 7.36–7.28 (m, 1H). ^{13}C NMR (100 MHz, CDCl_3) δ (ppm): 143.5, 141.3, 140.4, 137.6, 133.6, 129.9, 125.6, 123.9, 120.4, 118.9, 110.0, 109.9. MS (EI): m/z 484.88 [M^+]. Anal. calcd for $\text{C}_{36}\text{H}_{24}\text{N}_2$ (%): C 89.18, H 4.89, N 5.93; found: C 89.23, H 4.99, N 5.78.

1,3-bis(9-phenyl-9H-carbazol-3-yl)benzene (PBCz): **PBCz** was synthesized according to the same procedure as for **BCzPh** by using 1,3-dibromophenyl (1.13 g, 4.81 mmol) and 9-phenyl-9H-carbazol-3-ylboronic acid (3.03 g, 10.56 mmol). **PBCz** was afforded as a white solid (2.23 g, 82.9%). ^1H NMR (400 MHz, CDCl_3) δ (ppm): 8.45 (s, 2H) 8.23 (d, $J = 8.0\text{ Hz}$, 2H) 8.05 (s, 2H) 7.76 (d, $J = 8.0\text{ Hz}$, 2H) 7.71 (d, $J = 8.0\text{ Hz}$, 2H) 7.66–7.55 (m, 9H) 7.54–7.38 (m, 8H), 7.35–7.27 (m, 2H). ^{13}C NMR (400 MHz, CDCl_3) δ (ppm): 142.6, 141.4, 140.5, 137.6, 133.4, 129.9, 129.3, 127.5, 127.1, 126.5, 126.1, 125.6, 123.8, 123.5, 120.4, 120.1, 119.0, 110.1, 109.9. MS (EI): m/z 560.65 [M^+]. Anal. calcd for $\text{C}_{48}\text{H}_{32}\text{N}_2$ (%): C 89.97, H 5.03, N 5.00; found: C 90.00, H 5.08, N 4.92.

3,3'-bis(9-phenyl-9H-carbazol-3-yl)biphenyl (CTP-1): **CTP-1** was synthesized according to the same procedure as for **BCzPh** by using 3,3'-dibromodiphenyl (1.50 g, 4.81 mmol) and 9-phenyl-9H-carbazol-3-ylboronic acid (3.03 g, 10.56 mmol). **CTP-1** was afforded as a white solid (2.61 g, 85.5%). ^1H NMR (400 MHz, CDCl_3) δ (ppm): 8.43 (s, 2H) 8.21 (d, $J = 8.0\text{ Hz}$, 2H) 8.03 (s, 2H) 7.76–7.70 (m, 4H) 7.68 (d, $J = 8.0\text{ Hz}$, 2H) 7.64–7.55 (m, 10H) 7.51–7.37 (m, 8H), 7.33–7.26 (m, 2H). ^{13}C NMR (400 MHz, CDCl_3) δ (ppm): 142.6, 142.0, 141.4, 140.5, 137.6, 133.4, 129.9, 129.3, 129.9, 129.3, 127.5, 127.1, 126.5, 126.4, 126.2, 125.7, 125.6, 110.1, 109.9. MS (EI): m/z 636.52 [M^+]. Anal. calcd for $\text{C}_{48}\text{H}_{32}\text{N}_2$ (%): C 90.54, H 5.07, N 4.40; found: C 90.54, H 5.50, N 4.46.

Acknowledgements

We are grateful to the assistance of Dr. Cheng Zhong in molecular simulation. We acknowledge financial support from the Natural Science Foundation of China (Nos. 21202114, 21161160446, 61036009, and 61177016), the National High-Tech Research Development Program (No. 2011AA03A110), and the Natural Science Foundation of

Jiangsu Province (No. BK2010003). This is also a project funded by the Priority Academic Program Development of Jiangsu Higher Education Institutions (PAPD) and by the Research Supporting Program of Suzhou Industrial Park.

Appendix A. Supplementary material

Supplementary data associated with this article can be found, in the online version, at <http://dx.doi.org/10.1016/j.orgel.2014.03.028>.

References

- [1] K.R.J. Thomas, J.T. Lin, Y.-T. Tao, C.-W. Ko, *J. Am. Chem. Soc.* 123 (2001) 9404.
- [2] J. Li, A.C. Grimsdale, *Chem. Soc. Rev.* 39 (2010) 2399.
- [3] H.U. Kim, D. Mi, J.-H. Kim, J.B. Park, S.C. Yoon, U.C. Yoon, D.-H. Hwang, *Sol. Energy Mater. Sol. Cells*. 105 (2012) 6.
- [4] H. Uoyama, K. Goushi, K. Shizu, H. Nomura, C. Adachi, *Nature* 492 (2012) 234.
- [5] A. Hagfeldt, G. Boschloo, L. Sun, L. Kloo, H. Pettersson, *Chem. Rev.* 110 (2010) 6595.
- [6] M.A. Baldo, D.F. O'Brien, Y. You, A. Shoustikov, S. Sibley, M.E. Thompson, S.R. Forrest, *Nature* 395 (1998) 151.
- [7] M.A. Baldo, S. Lamansky, P.E. Burrows, M.E. Thompson, S.R. Forrest, *Appl. Phys. Lett.* 75 (1999) 4.
- [8] J. Bin, N. Cho, J. Hong, *Adv. Mater.* 24 (2012) 2911.
- [9] M.-H. Tsai, H.-W. Lin, H.-C. Su, T.-H. Ke, C.-C. Wu, F.-C. Fang, Y.-L. Liao, K.-T. Wong, C.-I. Wu, *Adv. Mater.* 18 (2006) 1216.
- [10] C.W. Lee, J.Y. Lee, *Adv. Mater.* 25 (2013) 5450.
- [11] E. Mondal, W.-Y. Huang, Y.-H. Chen, M.-H. Cheng, K.-T. Wong, *Chem. Eur. J.* 19 (2013) 10563.
- [12] C. Han, L. Zhu, F. Zhao, Z. Zhang, J. Wang, Z. Deng, H. Xu, J. Li, D. Ma, P. Yan, *Chem. Commun.* 50 (2014) 2670.
- [13] D. Yu, F. Zhao, C. Han, H. Xu, J. Li, Z. Zhang, Z. Deng, D. Ma, P. Yan, *Adv. Mater.* 24 (2012) 509.
- [14] W.S. Jeon, T.J. Park, S.Y. Kim, R. Pode, J. Jang, J.H. Kwon, *Org. Electron.* 10 (2009) 240.
- [15] R.J. Holmes, S.R. Forrest, Y.-J. Tung, R.C. Kwong, J.J. Brown, S. Garon, M.E. Thompson, *Appl. Phys. Lett.* 82 (2003) 2422.
- [16] Y. Divayana, X.W. Sun, *Phys. Rev. Lett.* 99 (2007) 143003.
- [17] S. Reineke, F. Lindner, G. Schwartz, N. Seidler, K. Walzer, B. Lüssem, K. Leo, *Nature* 459 (2009) 234.
- [18] Q. Wang, D. Ma, *Chem. Soc. Rev.* 39 (2010) 2387.
- [19] Y.H. Son, M.J. Park, Y.J. Kim, J.H. Yang, J.S. Park, J.H. Kwon, *Org. Electron.* 14 (2013) 1183.
- [20] N. Sun, Q. Wang, Y. Zhao, Y. Chen, D. Yang, F. Zhao, J. Chen, D. Ma, doi: 10.1002/adma.201304779.
- [21] C.-H. Chang, Y.-H. Lin, C.-C. Chen, C.-K. Chang, C.-C. Wang, L.-S. Chen, W.-W. Wu, Y. Chi, *Org. Electron.* 11 (2009) 1235.
- [22] H.-H. Chou, Y.-H. Chen, C.-C. Chang, C.-Y. Liao, C.-H. Cheng, *ACS Appl. Mater. Interfaces*. 5 (2013) 6168.
- [23] J.-H. Jou, S.-M. Shen, C.-R. Lin, Y.-S. Wang, Y.-C. Chou, S.-Z. Chen, Y.-C. Jou, *Org. Electron.* 12 (2011) 865.
- [24] G. Zhou, Q. Wang, C.L. Ho, W.Y. Wong, D. Ma, L. Wang, *Chem. Commun.* 24 (2009) 3574.
- [25] D. Volyniuk, V. Cherpak, P. Stakhira, B. Minaev, G. Baryshnikov, M. Chapran, A. Tomkeviciene, J. Keruckas, J.V. Grazulevicius, *J. Phys. Chem. C* 117 (2013) 22534.
- [26] Y.-S. Park, S. Lee, K.-H. Kim, S.-Y. Kim, J.-H. Lee, J.-J. Kim, *Adv. Funct. Mater.* 23 (2013) 4914.
- [27] K. Masui, H. Nakanotani, C. Adachi, *Org. Electron.* 14 (2013) 2721.
- [28] S. Huang, Q. Zhang, Y. Shiota, T. Nakagawa, K. Kuwabara, K. Yashizawa, C. Adachi, *J. Chem. Theory Comput.* 9 (2013) 3872.
- [29] S. Su, C. Cai, J. Kido, *Chem. Mater.* 23 (2011) 274.
- [30] Y. Tao, C. Yang, J. Qin, *Chem. Soc. Rev.* 40 (2011) 2943.
- [31] A. Chaskar, H.-F. Chen, K.-T. Wong, *Adv. Mater.* 23 (2011) 3876.
- [32] L. Xiao, Z. Chen, B. Qu, J. Luo, S. Kong, Q. Gong, *Adv. Mater.* 23 (2011) 926.
- [33] A. Wada, T. Yasuda, Q. Zhang, Y.S. Yang, I. Takasu, S. Enomoto, C. Adachi, *J. Mater. Chem. C* 1 (2013) 2404.
- [34] H. Inomata, K. Goushi, T. Masuko, T. Konno, T. Imai, H. Sasabe, J.J. Brown, C. Adachi, *Chem. Mater.* 16 (2004) 1285.
- [35] S.-J. Su, H. Sasabe, T. Takeda, J. Kido, *Chem. Mater.* 20 (2008) 1691.
- [36] T. Nishimoto, T. Yasuda, S.Y. Lee, R. Kondo, C. Adachi, *Mater. Horiz.* doi: 10.1039/C3MH00079F.
- [37] Q. Li, L.-S. Cui, C. Zhong, X.-D. Yuan, S.-C. Dong, Z.-Q. Jiang, L.-S. Liao, *Dyes Pigments* 101 (2014) 142.
- [38] H. Sasabe, H. Nakanishi, Y. Watanabe, S. Yano, M. Hirasawa, Y.-J. Pi, J. Kido, *Adv. Funct. Mater.* 23 (2013) 5550.
- [39] S. Lee, K.-H. Kim, D. Limbach, Y.-S. Park, J.-J. Kim, *Adv. Funct. Mater.* 23 (2013) 4105.
- [40] C. Fang, Y. Chen, Z. Liu, Z. Jiang, C. Zhang, D. Ma, J. Qin, C. Yang, *J. Mater. Chem. C* (2013) 463.
- [41] I. Avilov, P. Marsal, J.-L. Brédas, D. Beljonne, *Adv. Mater.* 16 (2004) 1624.
- [42] J. Wu, S.-X. Wu, Y. Wu, Y.-H. Kan, Y. Geng, Z.-M. Su, *Phys. Chem. Chem. Phys.* 15 (2013) 2351.
- [43] C. Han, Z. Zhang, H. Xu, S. Yue, J. Li, P. Yan, Z. Deng, Y. Zhao, P. Yan, S. Liu, *J. Am. Chem. Soc.* 134 (2012) 19179.
- [44] C. Han, Z. Zhang, H. Xu, G. Xie, J. Li, Y. Zhao, Z. Deng, S. Liu, P. Yan, *Chem. Eur. J.* 19 (2013) 141.
- [45] S. Gong, X. He, Y. Chen, Z. Jiang, D. Ma, J. Qin, C. Yang, *J. Mater. Chem. C* 22 (2012) 2894.
- [46] L.-S. Cui, Y. Liu, X.-D. Yuan, Q. Li, Z.-Q. Jiang, L.-S. Liao, *J. Mater. Chem. C* 1 (2013) 8177.
- [47] Y. Liu, L.-S. Cui, X.-M. Xu, X.-B. Xiao, D.-Y. Zhou, Z.-K. Wang, Z.-Q. Jiang, L.-S. Liao, *J. Mater. Chem. C*, doi: 10.1039/C3TC32301C.
- [48] L.-S. Cui, S.-C. Dong, Y. Liu, Q. Li, Z.-Q. Jiang, L.-S. Liao, *J. Mater. Chem. C* 1 (2013) 3967.
- [49] R.J. Holmes, B.W. Forrest, S.R. Ren, X. Li, M.E. Thompson, *Appl. Phys. Lett.* 18 (2003) 3818.
- [50] S. Salman, D. Kim, V. Coropceanu, J.-L. Brédas, *Chem. Mater.* 23 (2011) 5223.
- [51] D. Kim, V. Coropceanu, J.-L. Brédas, *J. Am. Chem. Soc.* 133 (2011) 1789.
- [52] C. Cai, S.-J. Su, T. Chiba, H. Sasabe, Y.-J. Pu, K. Nakayama, J. Kido, *Org. Electron.* 12 (2011) 843.
- [53] S. Chen, G. Tan, W.-Y. Wong, H.-S. Kwok, *Adv. Funct. Mater.* 21 (2011) 3785.
- [54] S.R. Forrest, D.D.C. Bradley, M.E. Thompson, *Adv. Mater.* 15 (2003) 1043.